JP Journal of Heat and Mass Transfer

Published Online: May 2016
http://dx.doi.org/10.17654/HM013020161
Volume 13, Number 2, 2016, Pages 161-181 **ISSN: 0973-5763**

HEAT AND MASS TRANSFER EFFECT ON MOVING VERTICAL PLATE WITH VARIABLE TEMPERATURE AND MASS DIFFUSION IN THE PRESENCE OF HALL EFFECT

R. Muthucumaraswamy and K. Muthuracku Alias Prema

Department of Applied Mathematics
Sri Venkateswara College of Engineering
Pennalur, Sriperumbudur Taluk - 602117
India
e-mail: msamy@svce.ac.in
kmprema66@yahoo.co.in

Abstract

This paper analyzes the effects of radiation on unsteady hydromagnetic free convection flow and heat mass transfer past an infinite vertical plate. The flow in the fluid is induced due to uniform motion of the plate. At time $t' > 0$, the plate is linearly accelerated with a velocity $u = u_0$ in its own plane. And at the same time, plate temperature and concentration levels near the plate raised linearly with time *t*. Exact solutions for the dimensionless governing coupled, non-linear boundary layer partial differential equations are solved by using Laplace transformation technique. The solutions are in terms of exponential and complementary error function. The results obtained are presented graphically for both axial and transverse velocity. The numerical values of velocity fields are studied for different parameters

Received: June 2, 2015; Accepted: June 16, 2015

Keywords and phrases: Hall effect, accelerated, vertical plate, temperature, mass diffusion.

Communicated by E. Thandapani; Editor: Far East Journal of Mathematical Sciences (FJMS): Published by Pushpa Publishing House.

such as Hall parameter (m), Hartmann number (M), rotation parameter (Ω), thermal radiation parameter (R), Schmidt number (Sc), thermal Grashof number (Gr) and mass Grashof number (Gc). An imposed rotation parameter Ω satisfying $\Omega = \frac{M^2 m}{1+m^2}$, the transverse motion (transverse to main flow) disappears and the fluid moves in the direction of the plate only. The effect of concentration profiles and the effect of temperature profiles were also presented graphically.

1. Introduction

Aboeldahab and Elbarbary [1] studied Hall current effect on magnetohydrodynamic free convection flow past a semi-infinite vertical plate with mass transfer. Abramowitz and Stegun [2] are using handbook of mathematical functions with formulas, graphs and mathematical tables. Deka and Das [3] have considered radiation effects on free convection flow near a vertical plate with ramped wall temperature. Hetnarski [4] examined an algorithm for generating some inverse Laplace transforms of exponential form. Jonah Philliph et al. [5] investigated MHD rotating heat and mass transfer free convective flow past an exponentially accelerated isothermal plate with fluctuating mass diffusion. Kafousias and Raptis [6] examined mass transfer and free convection effects on the flow past an accelerated vertical infinite plate with variable suction or injection. The effect of Hall currents on the magnetohydrodynamic boundary layer flow past a semi-infinite flat plate was carried out by Katagiri [7]. Jana et al. [8] studied effects of rotation and radiation on the hydrodynamic flow past an impulsively started vertical plate with ramped plate temperature. Muthucumaraswamy and Ganesan [9] have considered radiation effects on flow past an impulsively started infinite vertical plate with variable temperature. Muthucumaraswamy and Kumar [10] considered heat and mass transfer effects on moving vertical plate in the presence of thermal radiation. Muthucumaraswamy et al. [11] considered unsteady flow past an accelerated infinite vertical plate with variable temperature and mass diffusion. Hall effects on magnetohydrodynamic free convection about a semi-infinite

vertical flat plate were studied by Pop and Watanabe [12]. Nandkeolyar et al. [13] considered exact solutions of unsteady MHD free convection in a heat absorbing fluid flow past a flat plate with ramped wall temperature. Raptis et al. [14] have considered hydromagnetic free convection flow past an accelerated vertical infinite plate with variable suction and heat flux. The numerical solution of heat equation using the finite difference approximations is given by Recktenwald [15]. Shanker and Kishan [16] analyzed the effects of mass transfer on the MHD flow past an impulsively started infinite vertical plate with variable temperature or constant heat flux. Yilmaz et al. [17] were studied energy correlation of heat transfer and enhancement efficiency in decaying swirl flow.

2. Formulation of the Problem and its Solution

Consider the unsteady MHD flow of an infinite vertical plate with variable temperature and uniform mass diffusion. A magnetic field of uniform strength Bo is applied transversely to the plate. The flow is assumed to be in x'-direction which is taken along the vertical plate in the upward direction. The z-axis is taken to be normal to the plate. Initially, at time $t' \le 0,$ both the fluid and plate are at rest and at uniform temperature T'_∞ and the concentration of the fluid near the plate are assumed to be C'_∞. At time $t' > 0,$ the plate starts moving with a velocity $u = u_0$ in its own plane and the concentration from the plate is raised to C'_w and temperature of the plate is raised or lowered to $T' = T'_\infty + (T'_w - T'_\infty)At'.$ By usual Boussinesq's approximation for unsteady flow is governed by the following set of equations:

Equation of momentum:

$$\frac{\partial u}{\partial t'} - 2\Omega' v = \vartheta \frac{\partial^2 u}{\partial z^2} - \frac{1}{\rho}\frac{\partial p}{\partial x} + g + \frac{B_0}{\rho} j_y, \tag{1}$$

$$\frac{\partial v}{\partial t'} + 2\Omega' u = \vartheta \frac{\partial^2 v}{\partial z^2} - \frac{B_0}{\rho} j_x. \tag{2}$$

Equation of energy:

$$\rho C_p \frac{\partial T'}{\partial t'} = k \frac{\partial^2 T'}{\partial z^2} - \frac{\partial q_r}{\partial z}. \tag{3}$$

Equation of mass diffusion:

$$\frac{\partial C'}{\partial t'} = D \frac{\partial^2 C'}{\partial z^2}, \tag{4}$$

where T' is the fluid temperature, C' is the concentration, t' is the time, D is the diffusion term.

Since there is no large velocity gradient here, the viscous term in equation (1) vanishes for small and hence for the outer flow, beside there is no magnetic field along x-direction gradient, so we have

$$0 = -\frac{\partial p}{\partial x} - \rho_\infty g. \tag{5}$$

By eliminating the pressure term from equations (1) and (5), we obtain

$$\frac{\partial u}{\partial t'} - 2\Omega' v = \vartheta \frac{\partial^2 u}{\partial z^2} + (\rho_\infty - \rho) g + \frac{B_0}{\rho} j_y. \tag{6}$$

The Boussinesq approximation gives

$$\rho_\infty - \rho = \rho_\infty \beta (T' - T'_\infty) + \rho_\infty \beta^* (C' - C'_\infty). \tag{7}$$

On using (7) in equation (6) and noting that ρ_∞ is approximately equal to 1, the momentum equation reduces to

$$\frac{\partial u}{\partial t'} - 2\Omega' v = \vartheta \frac{\partial^2 u}{\partial z^2} + \frac{B_0}{\rho} j_y + g\beta (T' - T'_\infty) + g\beta^* (C' - C'_\infty), \tag{8}$$

where ρ is the density, ϑ is the kinematic viscosity, u and v are fluid velocity components, g is the acceleration due to gravity, C_p is the specific heat at constant pressure, q_r is the radiative heat flux in the z-direction, k is thermal conductivity, β is the volumetric coefficient of thermal expansion, β^* is the volumetric coefficient of expansion with concentration.

The generalized Ohm's law, on taking Hall currents into account and neglecting ion-slip and thermo-electric effect, is

$$\vec{j} + \frac{\omega_e \tau_e}{B_0}(\vec{j} \times \vec{B}) = \sigma(\vec{E} + \vec{q} \times \vec{B}), \tag{9}$$

where $\vec{j}$ is the current density vector, $\vec{q}$ is the velocity vector, $\vec{B}$ is the magnetic field vector, $\vec{E}$ is the electric field vector, ω_e is the cyclotron frequency, σ is the electrical conductivity of the fluid and τ_e is the collision time of electron.

Equation (9) gives

$$j_x - mj_y = \sigma v B_0, \tag{10}$$

$$j_y + mj_x = -\sigma u B_0, \tag{11}$$

where $m = \omega_e \tau_e$ is the Hall parameter. Solving (10) and (11) for j_x and j_y, we have

$$j_x = \frac{\sigma B_0}{1 + m^2}(v - mu), \tag{12}$$

$$j_y = \frac{\sigma B_0}{1 + m^2}(u + mv). \tag{13}$$

On the use of (12) and (13), the momentum equations (8) and (2) become

$$\frac{\partial u}{\partial t'} = \vartheta \frac{\partial^2 u}{\partial z^2} + 2\Omega' v - \frac{\sigma B_0^2 (u + mv)}{\rho(1 + m^2)} + g\beta(T' - T'_\infty) + \rho\beta^*(C' - C'_\infty), \tag{14}$$

$$\frac{\partial v}{\partial t'} = \vartheta \frac{\partial^2 v}{\partial z^2} - 2\Omega' u + \frac{\sigma B_0^2 (mu - v)}{\rho(1 + m^2)}. \tag{15}$$

Here u is the axial velocity (along the direction of the plate) and v is the transverse velocity (transverse to the main flow), the initial and boundary conditions are given by

$$\left.\begin{aligned} &u = 0,\ v = 0,\ T' = T'_\infty,\ C' = C'_\infty,\ t' \le 0,\ \forall z \\ &t' > 0,\ u = u_0,\ v = 0,\ T' = T'_\infty + (T'_w - T'_\infty)At',\ C' = C'_w \text{ at } z = 0 \\ &u \to 0,\ v \to 0,\ T' \to T'_\infty,\ C' \to C'_\infty \text{ as } z \to \infty \end{aligned}\right\}, \quad (16)$$

where $A = \dfrac{u_0^2}{\gamma}$.

The local radiant for the case of an optically thin gray gas is expressed by

$$\frac{\partial q_r}{\partial z} = -4a^*\sigma(T'^4_\infty - T'^4). \quad (17)$$

It is assumed that the temperature differences within the flow are sufficiently small such that T'^4 may be expressed as a linear function of the temperature. This is accomplished by expanding T'^4 in a Taylor series about T'_∞ and neglecting higher-order terms, thus

$$T'^4 \cong 4T'^3_\infty T' - 3T'^4_\infty. \quad (18)$$

By using equations (17) and (18), equation (3) reduces to

$$\rho C_p \frac{\partial T'}{\partial t'} = k\frac{\partial^2 T'}{\partial z^2} + 16a^*\sigma T'^3_\infty (T'_\infty - T'). \quad (19)$$

Let us introducing the following non-dimensional quantities:

$$\left.\begin{aligned} &U = \frac{u}{u_0},\ V = \frac{v}{u_0},\ Z = \frac{zu_0}{\gamma},\ t = \frac{t'u_0^2}{\gamma},\ \Omega = \frac{\Omega'\gamma}{u_0^2},\ M^2 = \frac{\Omega\sigma B_0^2\gamma}{2\rho u_0^2}, \\ &Gr = \frac{g\beta\gamma(T'_w - T'_\infty)}{u_0^3},\ Gc = \frac{g\beta^*\gamma(C'_w - C'_\infty)}{u_0^3},\ \theta = \frac{T' - T'_\infty}{T'_w - T'_\infty}, \\ &C = \frac{C' - C'_\infty}{C'_w - C'_\infty},\ Pr = \frac{\rho C_p}{k},\ Sc = \frac{\nu}{D},\ R = \frac{16a^*\sigma\gamma^2 T'^3_\infty}{ku_0^2} \end{aligned}\right\}, \quad (20)$$

where Ω is the rotation parameter, Gr is the thermal Grashof number, Gc is

the mass Grashof number, *Pr* is the Prandtl number, *Sc* is the Schmidt number, *R* is the radiation parameter, *t* is the dimensionless time, *u* and *v* are the dimensionless velocities, *m*-Hall parameter, *M*-Hartmann number, *C* is the dimensionless concentration and θ is the dimensionless temperature.

Using these boundary conditions in above equations, we obtain the following dimensionless form of the governing equations:

$$\frac{\partial U}{\partial t} = \frac{\partial^2 U}{\partial Z^2} + 2\Omega V - \frac{2M^2(U + mV)}{1 + m^2} + Gr\theta + GcC, \tag{21}$$

$$\frac{\partial V}{\partial t} = \frac{\partial^2 V}{\partial Z^2} - 2\Omega U + \frac{2M^2(mU - V)}{1 + m^2}, \tag{22}$$

$$\frac{\partial \theta}{\partial t} = \frac{1}{Pr}\frac{\partial^2 \theta}{\partial Z^2} - \frac{R}{Pr}\theta, \tag{23}$$

$$\frac{\partial C}{\partial t} = \frac{1}{Sc}\frac{\partial^2 C}{\partial Z^2}. \tag{24}$$

The boundary conditions for corresponding order are

$$\left.\begin{array}{l} U = 0,\ V = 0,\ \theta = 0,\ C = 0 \text{ at } t \le 0 \text{ for all } Z \\ t > 0,\ U = 1,\ V = 0,\ \theta = t,\ C = 1 \text{ at } Z = 0 \\ U \to 0,\ V \to 0,\ \theta \to 0,\ C \to 0 \text{ as } Z \to \infty \end{array}\right\}. \tag{25}$$

Now equations (21) and (22) and boundary conditions (25) can be combined to give

$$\frac{\partial F}{\partial t} = \frac{\partial^2 F}{\partial Z^2} - aF + Gr\theta + GcC, \text{ where } a = \frac{2M^2}{1 + m^2} + 2i\left(\Omega - \frac{M^2 m}{1 + m^2}\right), \tag{26}$$

$$\frac{\partial \theta}{\partial t} = \frac{1}{Pr}\frac{\partial^2 \theta}{\partial Z^2} - \frac{R}{Pr}\theta, \tag{27}$$

$$\frac{\partial C}{\partial t} = \frac{1}{Sc}\frac{\partial^2 C}{\partial Z^2}. \tag{28}$$

The initial and boundary conditions in non-dimensional quantities are

$$\left.\begin{array}{l} F = 0,\ \theta = 0,\ C = 0 \text{ for all } Z,\ t \le 0 \\ t > 0,\ F = 1,\ \theta = t,\ C = 1 \text{ at } Z = 0 \\ F \to 0,\ \theta \to 0,\ C \to 0 \text{ as } Z \to \infty \end{array}\right\}, \tag{29}$$

where $F = U + iV$.

Equations (26), (27), (28), subject to the boundary conditions (29), are solved by the usual Laplace-transform technique and the solutions are derived as follows:

$$\begin{aligned} & F(Z, t) \\ & = (1 + a_1 - a_2)\left(\frac{1}{2}\right)[\exp(2\eta\sqrt{at})\,erfc(\eta + \sqrt{at}) + \exp(-2\eta\sqrt{at})\,erfc(\eta - \sqrt{at})] \\ & + a_1 d\left[\left(\frac{t}{2}\right)(\exp(2\eta\sqrt{at})\,erfc(\eta + \sqrt{at}) + \exp(-2\eta\sqrt{at})\,erfc(\eta - \sqrt{at})) \right. \\ & \left. - \left(\frac{\eta\sqrt{t}}{2\sqrt{a}}\right)(\exp(-2\eta\sqrt{at})\,erfc(\eta - \sqrt{at}) - \exp(2\eta\sqrt{at})\,erfc(\eta + \sqrt{at}))\right] \\ & - a_1 g[\exp(2\eta\sqrt{(a+d)t})\,erfc(\eta + \sqrt{(a+d)t}) \\ & + \exp(-2\eta\sqrt{(a+d)t})\,erfc(\eta - \sqrt{(a+d)t})] \\ & + a_2 h[\exp(2\eta\sqrt{(a+e)t})\,erfc(\eta + \sqrt{(a+e)t}) \\ & + \exp(-2\eta\sqrt{(a+e)t})\,erfc(\eta - \sqrt{(a+e)t})] \\ & - \frac{a_1}{2}[\exp(2\eta\sqrt{Prbt})\,erfc(\eta\sqrt{Pr} + \sqrt{bt}) + \exp(-2\eta\sqrt{Prbt})\,erfc(\eta\sqrt{Pr} - \sqrt{bt})] \\ & - a_1 d\left[\left(\frac{t}{2}\right)(\exp(2\eta\sqrt{Prbt})\,erfc(\eta\sqrt{Pr} + \sqrt{bt}) \right. \\ & \left. + \exp(-2\eta\sqrt{Prbt})\,erfc(\eta\sqrt{Pr} - \sqrt{bt})) \right. \\ & \left. - \left(\frac{\eta\sqrt{Pr}\sqrt{t}}{2\sqrt{b}}\right)(\exp(-2\eta\sqrt{Prbt})\,erfc(\eta\sqrt{Pr} - \sqrt{bt})\right. \end{aligned}$$

$$- \exp(2\eta\sqrt{Prbt})\,erfc(\eta\sqrt{Pr} + \sqrt{bt})\Big]$$

$$+ a_1 g[\exp(2\eta\sqrt{Pr(b+d)t})\,erfc(\eta\sqrt{Pr} + \sqrt{(b+d)t})$$

$$+ \exp(-2\eta\sqrt{Pr(b+d)t})\,erfc(\eta\sqrt{Pr} - \sqrt{(b+d)t})]$$

$$- a_2 h[\exp(2\eta\sqrt{Scet})\,erfc(\eta\sqrt{Sc} + \sqrt{et})$$

$$+ \exp(-2\eta\sqrt{Scet})\,erfc(\eta\sqrt{Sc} - \sqrt{et})] + a_2(erfc(\eta\sqrt{Sc})),$$

where $\eta = \dfrac{z}{2\sqrt{t}}$; $a_1 = \dfrac{Gr}{(1-Pr)d^2}$; $a_2 = \dfrac{Gc}{(Sc-1)e}$; $b = \dfrac{R}{Pr}$; $d = \dfrac{bPr-a}{1-Pr}$;

$e = \dfrac{a}{Sc-1}$; $g = \dfrac{\exp(dt)}{2}$; $h = \dfrac{\exp(et)}{2}$.

In order to get the physical insight into the problem, the numerical values of F have been computed from (19). While evaluating this expression, it is observed that the argument of the error function is complex and, hence, we have separated it into real and imaginary parts by using the following formula:

$$erf(a+ib) = erf(a) + \frac{\exp(-a^2)}{2a\pi}[1 - \cos(2ab) + i\sin(2ab)]$$

$$+ \frac{2\exp(-a^2)}{\pi}\sum_{n=1}^{\infty}\frac{\exp\left(-\dfrac{n^2}{4}\right)}{n^2+4a^2}[f_n(a,b) + ig_n(a,b)] + \in(a,b),$$

where $f_n = 2a - 2a\cosh(nb)\cos(2ab) + n\sinh(nab)\sin(2ab)$ and

$$g_n = 2a\cosh(nb)\sin(2ab) + n\sinh(nab)\cos(2ab),$$

$$|\in(a,b)| \approx 10^{-16}|erf(a+ib)|.$$

We have included the explanation of symbol $\in(a, b)$.

3. Results and Discussion

A set of numerical computations are carried out for parameters Ω, M, m,

R, *Gr*, *Gc*, *Sc*. The values of Prandtl number *Pr* are chosen 0.71 (air). The value of Schmidt number is chosen to represent water vapour $(Sc = 0.6)$. The numerical values of the axial and transverse velocity, temperature and concentration profiles are computed graphically. In Figure 1, the concentration profile at time $t = 0.2$ decreases with increase in the values of *Sc*. The temperature profiles are calculated for different values of thermal radiation parameter ($R = 0.2, 0.2, 2.0, 5.0$) and time ($t = 0.2, 0.6, 0.2, 0.2$) are shown in Figure 2. It is observed that the temperature increases with decreasing radiation parameter. It is observed from Figure 3 transverse velocity with minimum for $\Omega = M^2 m/(1+m^2)$ and increases as Ω increases. In Figure 4, the axial velocity profile for different Ω has been presented and it is observed that the primary velocity *U* falls when Ω are increased. Figures 5 and 6 represent the velocity profiles for various values of *m*. It is found that from Figure 5 due to an increase in the Hall parameter, *m*, there is rise in the transverse velocity components. It is observed from Figure 6 that the axial velocity rises due to increasing value of the Hall parameter *m*. Figure 7 shows that due to an increase in the Hartmann number *M*, the transverse velocity increases. From Figure 8, it is clear that the axial velocity increases with decreasing values of the Hartmann number (*M*). The effect of radiation parameter *R* on velocity profile is shown in Figures 9 and 10. Figure 9 shows that due to an increase in the radiation parameter, the transverse velocity increases. From Figure 10, it is clear that the axial velocity increases with decreasing values of radiation parameter. It is observed from Figure 11 that the transverse velocity increases with increasing values of *Gr*, *Gc*. In Figure 12, it is observed that the axial velocity increases with increasing values of the thermal Grashof number or mass Grashof number. In Figure 13, it is observed that the transverse velocity increases with increasing values of *Sc*. In Figure 14, it is observed that the axial velocity increases with decreasing values of Schmidt number (*Sc*). The velocity profiles for different values of time *t* are presented in Figures 15 and 16. It is observed that the axial velocity and transverse velocity increases with increasing values of *t*.

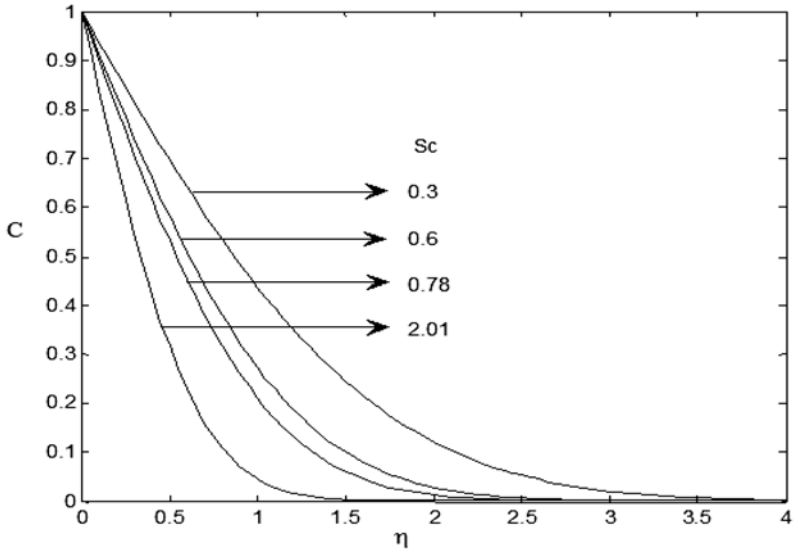

Figure 1. Concentration profiles for different values of *Sc* at time $t = 0.2$, it is observed that the concentration increases with decreasing values of the Schmidt number.

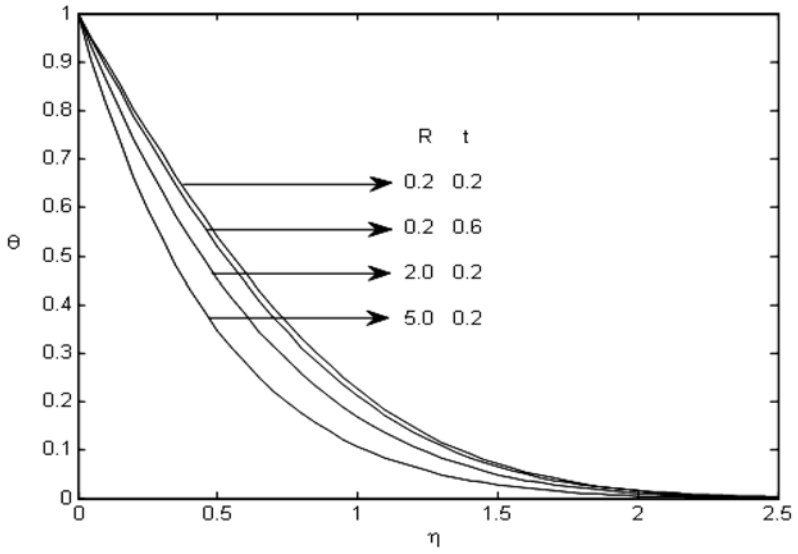

Figure 2. Temperature profiles for different values of *R* and *t*, the temperature increases with decreasing radiation parameter.

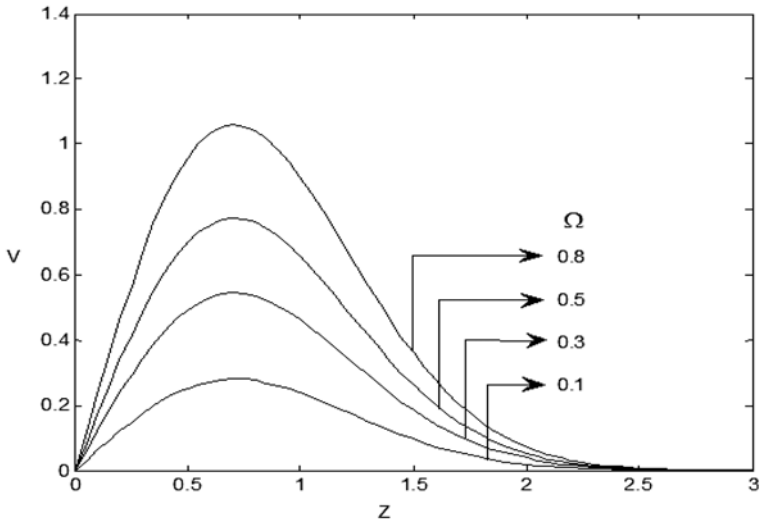

Figure 3. Transverse velocity profiles for several values of Ω when $Sc = 0.6$, $Pr = 0.71$, $t = 0.2$, $M = 0.5$, $m = 0.5$, $Gr = 5$, $Gc = 5$, $R = 5$, it is observed that the transverse velocity with minimum for $\Omega = M^2 m/(1+m^2)$ and increases as Ω increases.

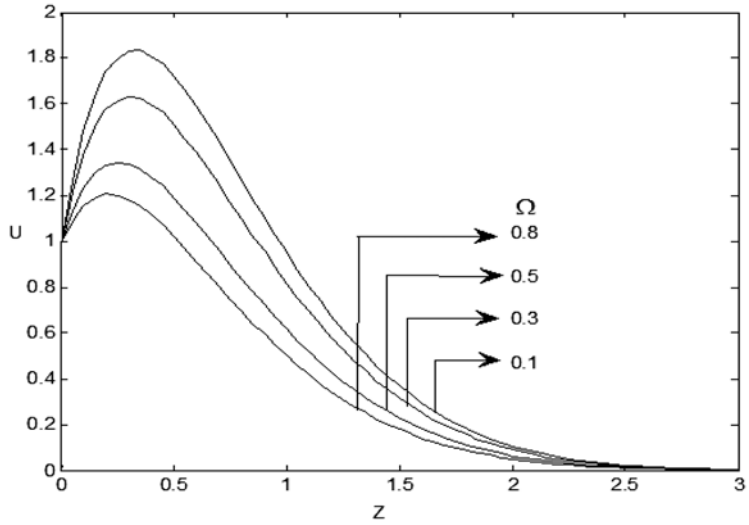

Figure 4. Axial velocity profiles for several values of Ω when $Sc = 0.6$, $Pr = 0.71$, $t = 0.2$, $M = 0.5$, $m = 0.5$, $Gr = 5$, $Gc = 5$, $R = 5$, it is further observed that the axial velocity U falls when Ω are increased.

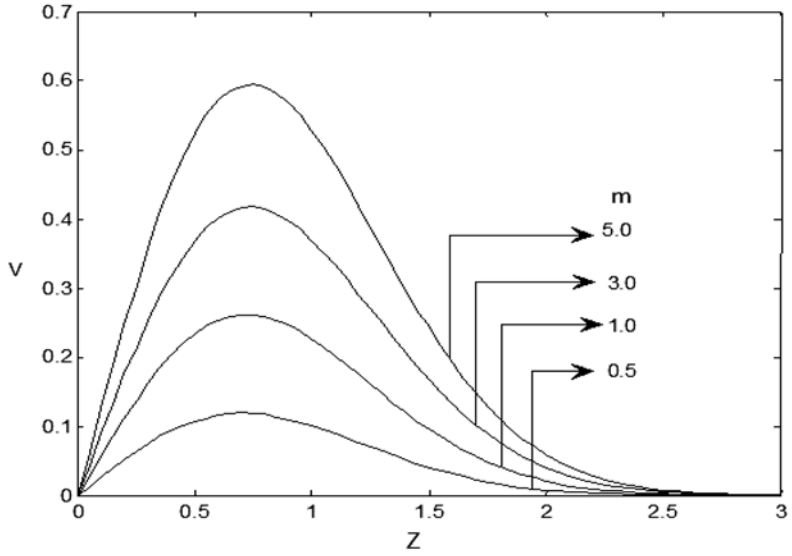

Figure 5. Transverse velocity profiles for several values of m when $Sc = 0.6$, $Pr = 0.71$, $t = 0.2$, $\Omega = 0.1$, $M = 0.5$, $Gr = 5$, $Gc = 5$, $R = 5$, due to an increase in the Hall parameter, m, there is rise in the transverse velocity components.

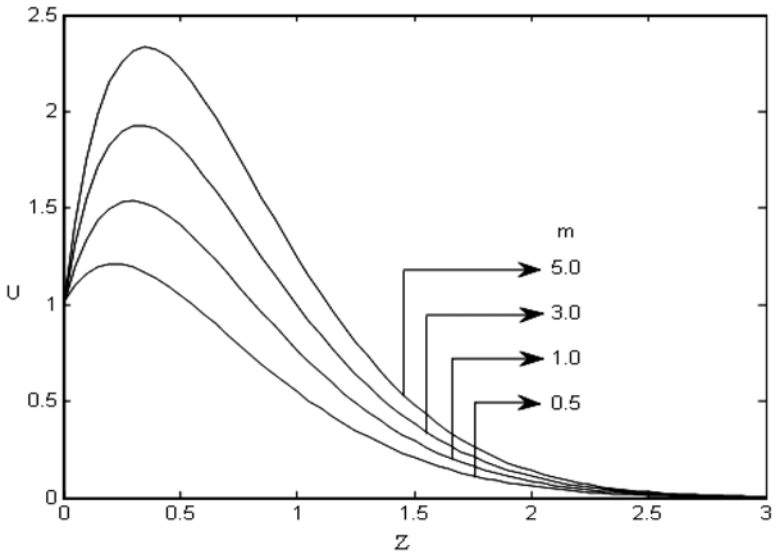

Figure 6. Axial velocity profiles for several values of m when $Sc = 0.6$, $Pr = 0.71$, $t = 0.2$, $\Omega = 0.1$, $M = 0.5$, $Gr = 5$, $Gc = 5$, $R = 5$, the axial velocity rises due to increasing value of the Hall parameter m.

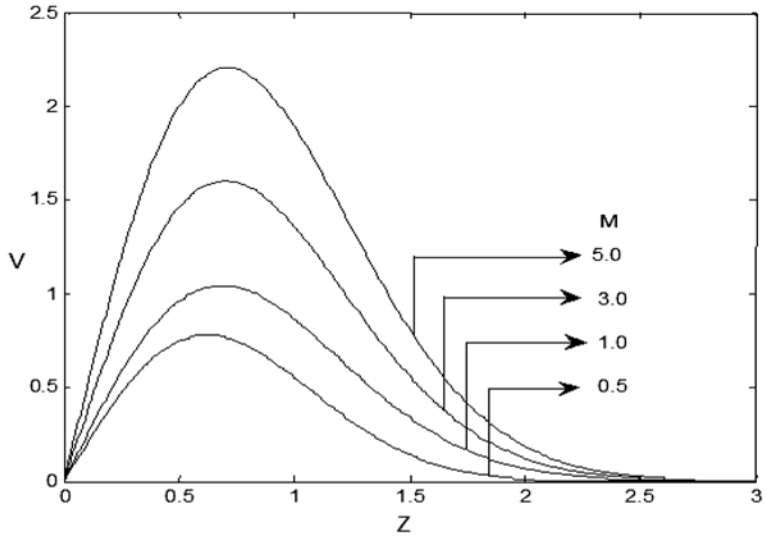

Figure 7. Transverse velocity profiles for several values of M when $Sc = 0.6$, $Pr = 0.71$, $t = 0.2$, $\Omega = 0.1$, $m = 0.5$, $Gr = 5$, $Gc = 5$, $R = 5$. It is observed that due to an increase in the Hartmann number M, the transverse velocity increases.

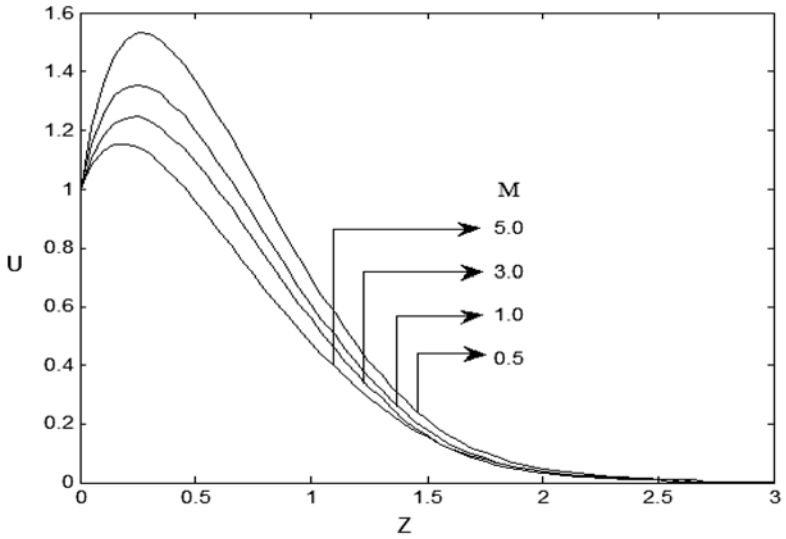

Figure 8. Axial velocity profiles for several values of M when $Sc = 0.6$, $Pr = 0.71$, $t = 0.2$, $\Omega = 0.1$, $m = 0.5$, $Gr = 5$, $Gc = 5$, $R = 5$. It is observed that the axial velocity increases with decreasing values of the Hartmann number (M).

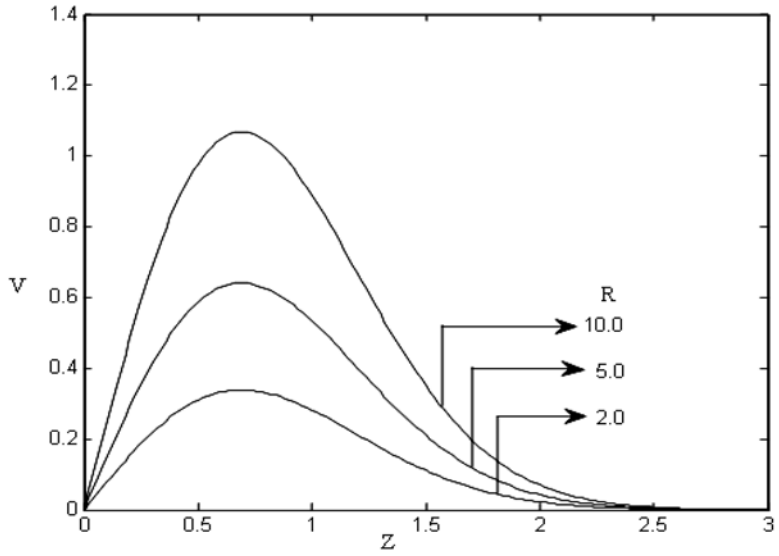

Figure 9. Transverse velocity profiles for several values of R when $Sc = 0.6$, $t = 0.2$, $Pr = 0.71$, $\Omega = 0.1$, $M = 0.5$, $m = 0.5$, $Gr = 5$, $Gc = 5$ due to an increase in the radiation parameter R, the transverse velocity increases.

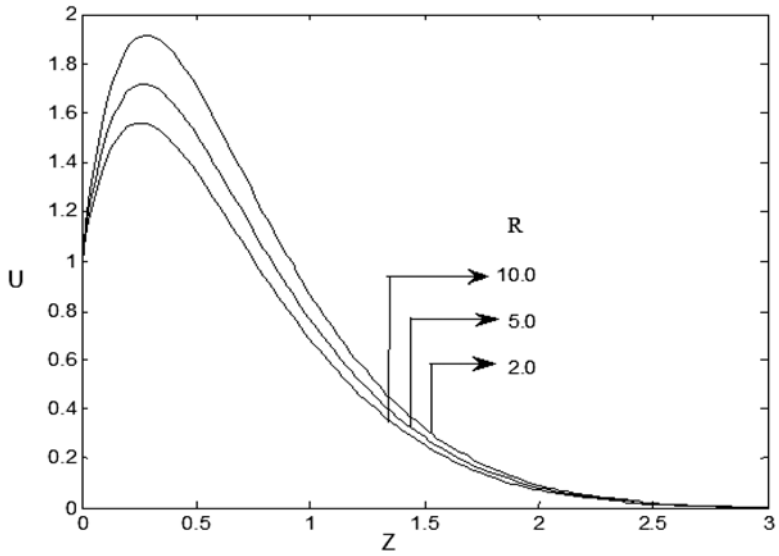

Figure 10. Axial velocity profiles for several values of R when $Sc = 0.6$, $Pr = 0.71$, $t = 0.2$, $\Omega = 0.1$, $M = 0.5$, $m = 0.5$, $Gr = 5$, the axial velocity increases decreasing values of the radiation parameter (R).

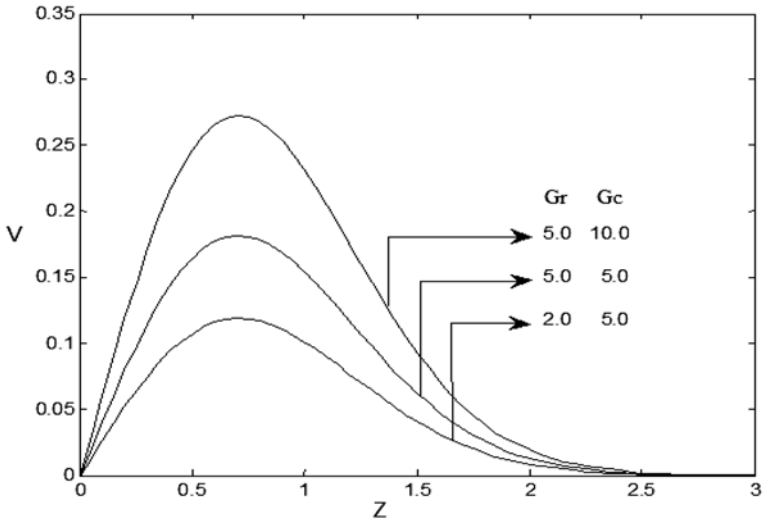

Figure 11. Transverse velocity profiles for several values of *Gr* and *Gc* when *Sc* = 0.6, *t* = 0.2, *Pr* = 0.71, Ω = 0.1, *M* = 0.5, *m* = 0.5, *R* = 5. It is observed that the transverse velocity increases with increasing values of the thermal Grashof number or mass Grashof number.

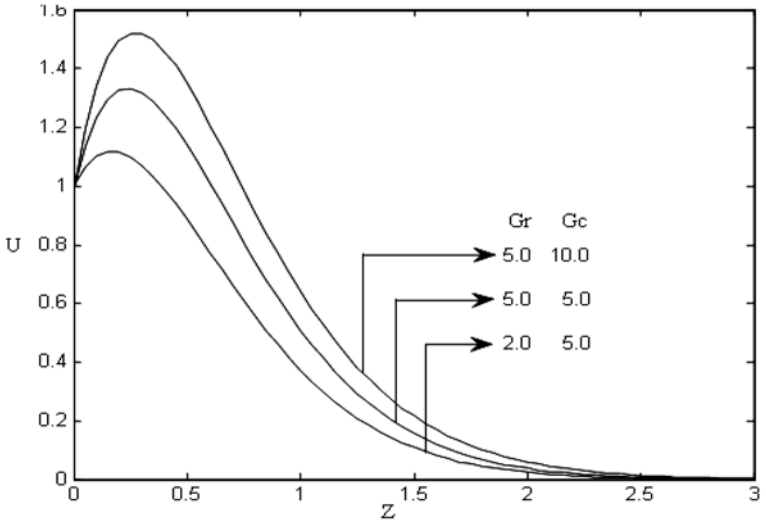

Figure 12. Axial velocity profiles for several values of *Gr* and *Gc* when *Sc* = 0.6, *Pr* = 0.71, *t* = 0.2, Ω = 0.1, *M* = 0.5, *m* = 0.5, *R* = 5. It is observed that the axial velocity increases with increasing values of the thermal Grashof number or mass Grashof number.

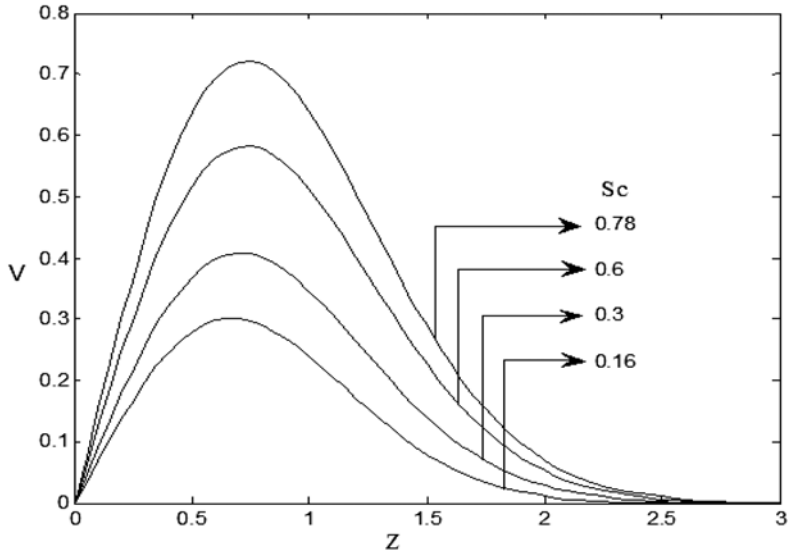

Figure 13. Transverse velocity profiles for several values of *Sc* when *Pr* = 0.71, *R* = 5, *t* = 0.2, Ω = 0.1, *M* = 0.5, *m* = 0.5, *Gr* = 5, *Gc* = 5 that the transverse velocity increases with increasing values of *Sc*.

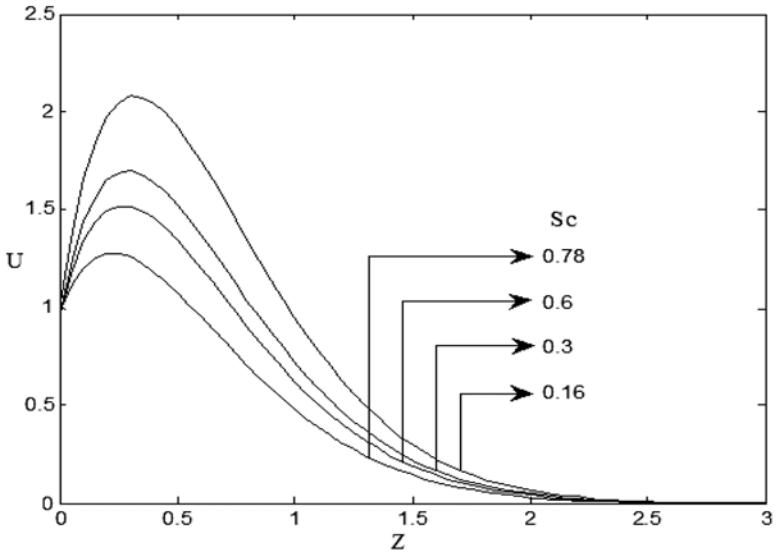

Figure 14. Axial velocity profiles for several values of *Sc* when *Pr* = 0.71, *R* = 5, *t* = 0.2, Ω = 0.1, *M* = 0.5, *m* = 0.5, *Gr* = 5, *Gc* = 5 that the axial velocity increases with decreasing values of Schmidt number of *Sc*.

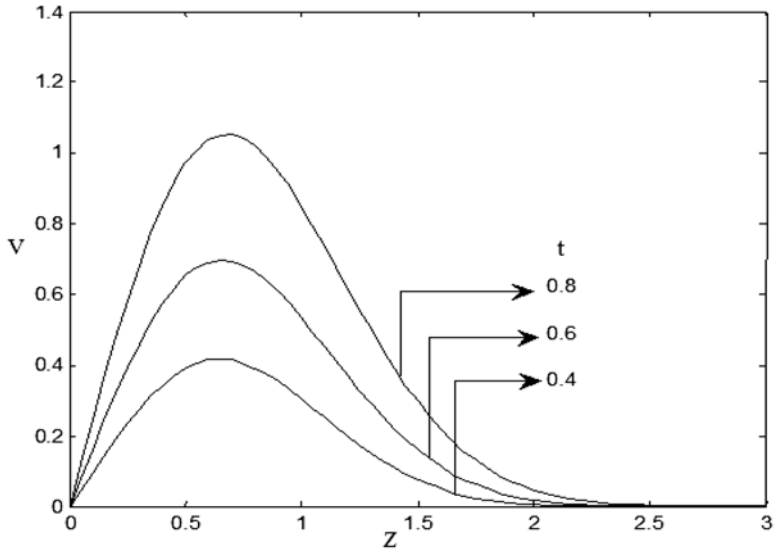

Figure 15. Transverse velocity profiles for several values of t when Pr = 0.71, R = 5, Sc = 0.6, Ω = 0.1, M = 0.5, m = 0.5, Gr = 5, Gc = 5. It is observed that the transverse velocity increases with increasing values of t.

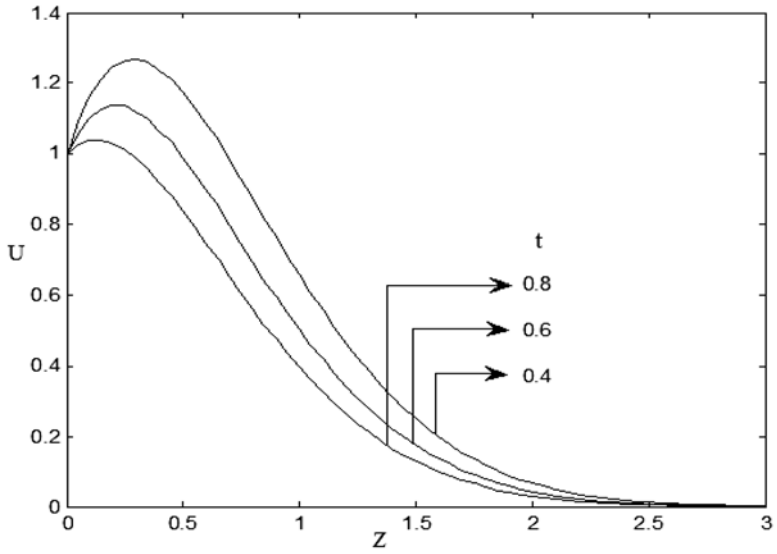

Figure 16. Axial velocity profiles for several values of t when Pr = 0.71, R = 5, Sc = 0.6, Ω = 0.1, M = 0.5, m = 0.5, Gr = 5, Gc = 5. It is observed that the axial velocity increases with increasing values of t.

4. Conclusion

Theoretical solution of an unsteady flow past an impulsively started infinite vertical plate in the presence of variable temperature and mass diffusion. The dimensional governing equations are solved by Laplace transform technique. The effect of different parameters like Hall parameter, Hartmann number, rotation parameter, radiation parameter, thermal Grashof number, mass Grashof number, Schmidt number are studied graphically. The conclusions of the study show that

- The concentration increases with decreasing values of the Schmidt number.
- The temperature increases with decreasing radiation parameter.
- The axial velocity rises due to increasing value of the Hall parameter, thermal Grashof number and mass Grashof number.
- The axial velocity u falls when Ω are increased, the velocity increases with decreasing values of the Hartmann number, the radiation parameter.
- Transverse velocity increases as Ω increases, due to an increase in the Hartmann number M, the Hall parameter, m, the radiation parameter R, Gr, Gc and Sc.

References

[1] E. M. Aboeldahab and E. M. E. Elbarbary, Hall current effect on magnetohydrodynamic free convection flow past a semi-infinite vertical plate with mass transfer, Int. J. Eng. Sci. 39 (2001), 1641-1652.

[2] B. M. Abramowitz and I. A. Stegun, Hand Book of Mathematical Functions with Formulas, Graphs and Mathematical Tables, U.S. Govt. Printing Office, Washington, 1964.

[3] R. K. Deka and S. K. Das, Radiation effects on free convection flow near a vertical plate with ramped wall temperature, Engineering 3 (2011), 1197-1206.

[4] R. B. Hetnarski, An algorithm for generating some inverse Laplace transforms of exponential form, ZAMP 26 (1975), 249-253.

[5] K. Jonah Philliph, M. C. Raju, A. J. Chamkha and S. V. K. Varma, MHD rotating heat and mass transfer free convective flow past an exponentially accelerated isothermal plate with fluctuating mass diffusion, Int. J. Indust. Math. 6(4) (2014), 297-306.

[6] N. G. Kafousias and A. Raptis, Mass transfer and free convection effects on the flow past an accelerated vertical infinite plate with variable suction or injection, Rev. Roum. Sci. Tech.- Mec. Apl. 26 (1981), 11-22.

[7] M. Katagiri, The effect of Hall currents on the magnetohydrodynamic boundary layer flow past a semi-infinite flat plate, J. Phys. Soc. Japan 27 (1969), 1051-1059.

[8] M. Jana, S. Das and R. N. Jana, Effects of rotation and radiation on the hydrodynamic flow past an impulsively started vertical plate with ramped plate temperature, Int. J. Appl. Inform. Sys. 3(4) (2012), 39-51.

[9] R. Muthucumaraswamy and P. Ganesan, Radiation effects on flow past an impulsively started infinite vertical plate with variable temperature, Int. J. Appl. Mech. Eng. 8 (2003), 125-129.

[10] R. Muthucumaraswamy and G. S. Kumar, Heat and mass transfer effects on moving vertical plate in the presence of thermal radiation, Theo. Appl. Mech. 31(1) (2004), 35-46.

[11] R. Muthucumaraswamy, M. Sundar Raj and V. S. A. Subramanian, Unsteady flow past an accelerated infinite vertical plate with variable temperature and mass diffusion, Int. J. Appl. Math. Mech. 5(6) (2009), 51-56.

[12] I. Pop and T. Watanabe, Hall effects on magnetohydrodynamic free convection about a semi-infinite vertical flat plate, Int. J. Eng. Sci. 32 (1994), 1903-1911.

[13] Raj Nandkeolyar, Mrutyunjay Das and Precious Sibanda, Exact solutions of unsteady MHD free convection in a heat absorbing fluid flow past a flat plate with ramped wall temperature, Boundary Value Problems 2013 (2013), 247.

[14] A. Raptis, G. J. Tzivanidis and C. P. Peridikis, Hydromagnetic free convection flow past an accelerated vertical infinite plate with variable suction and heat flux, Lett. Heat Mass Transfer 8 (1981), 137-143.

[15] G. W. Recktenwald, Finite difference approximations to the heat equation, Mech. Eng. 10 (2004), 1-27.

[16] B. Shanker and N. Kishan, The effects of mass transfer on the MHD flow past an impulsively started infinite vertical plate with variable temperature or constant heat flux, J. Energy Heat Mass Transfer 19 (1997), 273-278.

[17] M. Yilmaz, S. Yapici, O. Jomakli and O. N. Sara, Energy correlation of heat transfer and enhancement efficiency in decaying swirl flow, Heat Mass Transfer 38(4-5) (2002), 351-358.